

Scale-invariant multilevel Monte Carlo method

Sharana Kumar Shivanand^{a,*}, Bojana Rosić^b

^a *Institute of Scientific Computing, Technische Universität Braunschweig, Germany*

^b *Applied Mechanics and Data Analysis, University of Twente, Netherlands*

Abstract

In this paper, the scale-invariant version of the mean and variance multi-level Monte Carlo estimate is proposed. The optimization of the computation cost over the grid levels is done with the help of a novel normalized error based on t-statistic. In this manner, the algorithm convergence is made invariant to the physical scale at which the estimate is computed. The novel algorithm is tested on the linear elastic example, the constitutive law of which is described by material uncertainty including both heterogeneity and anisotropy.

Keywords: scale-invariant multilevel Monte Carlo method, mean and variance estimator, random tensor, anisotropy, bone, linear elasticity

1. Introduction

One of the major tasks in stochastic simulation is to efficiently propagate the uncertainty from the input to the system response, particularly in a high-dimensional random field scenario. For many years, the Monte Carlo method (MC) has remained the golden standard to solve stochastic problems [19, 9, 13]. However, this scheme is often practically unfeasible due to its slow convergence and a tremendous amount of computational effort. Therefore, recently, the scientific attention has shifted to a computationally more adequate sampling-based multilevel Monte Carlo method (MLMC). The success of MLMC lies in the refinement of the solution space such that the number of stochastic samples drastically decays with the grid refinement. Under appropriate conditions, this results in an overall reduction of the computational cost as compared to MC.

To the best of authors' knowledge, the MLMC is first introduced by [15] in the context of estimating multi-dimensional parameter-dependent integrals, and is further employed by [11] for solving Itô's stochastic ordinary differential equations in the computational finance application. Following this, the MLMC is extended to solve the linear elliptic PDEs describing the subsurface flow with in-homogeneous stochastic parameters [6, 2], whereas the extension to the random field scenario is studied in [6, 28]. The previously mentioned works are focusing on the approximation of the output response sample mean, and therefore are lacking full characterization of the probabilistic solution. Consequently, [20] studies the unbiased MLMC sample variance estimator which further is analysed in [3] on a class of elliptic random obstacle problems. An alternative MLMC variance estimator is introduced in [18] based on h-statistics [7, 21]. Though the estimation of other higher-

*Corresponding author.

E-mail address: s.shivanand@tu-bs.de

order moments such as skewness and kurtosis through MLMC is out of the scope of this paper, more literature on this can be found in [4, 18].

In the context of the implementation of the MLMC algorithm, the literature for both mean and variance estimation is focusing on the absolute error estimates or relative error estimates in the deterministic setting. However, such error estimates are not suitable for practical application as the stochastic algorithm convergence is dependent on the scale/magnitude of the quantity of interest. Hence, the performance comparison between different estimators or individual estimators on different scales cannot be done. To overcome this issue, in this article, we propose a scale-invariant error estimate based on t-statistic [27, 8]. The newly introduced relative error is of statistical nature and is used to normalize the sampling part of the MLMC algorithm. In other words, the error estimate can be used for an easier comparison of the MLMC mean and variance estimates to the corresponding MC ones; thus, improving the overall interpretability of the MLMC algorithm.

The other objective of this paper is to investigate the applicability of the scale-invariant MLMC method to linear elliptic problems described by stochastic parameters representing both heterogeneity and uncertain material symmetries. As an example, we consider the linear-elastic material model of the human femoral bone, the constitutive law of which is assumed to be uncertain. In particular, the bone material symmetry is described as uncertain due to lack of conclusive verification of the class of elastic symmetry the human femur belongs to [23, 17]. Hence, the entire elasticity tensor is constructed as random with predefined elastic symmetry in the mean (orthotropy [10] in this case) and purely arbitrary symmetries in each stochastic realization. Consequently, the positive-definite random elasticity matrices are modelled as matrix-valued random fields as proposed in [25, 26]. In this work, we restrict ourselves to material uncertainties only, assuming that the remaining model parametrization is deterministic. However, the numerical approach is general enough to be employed for other types of uncertainties as well.

The paper is organised as follows. In Section 2, we describe the model problem; the theoretical procedure of scale-invariant MC mean and variance estimates are elaborated in Section 2.1. Following this, in Section 3, the normalized version of MLMC mean and variance estimators are detailed. A deterministic and stochastic setting of the linear elastic material model along with the stochastic material modelling is given in Section 4. In Section 5, numerical results of the normalized MLMC and MC, when implemented on two-dimensional proximal femur are explained. Finally, the conclusions are drawn in Section 6.

2. Uncertainty Quantification

Let be given physical system occupying domain \mathcal{G} modelled by an equilibrium equation:

$$A(q, u) = f, \quad u(0) = u_0, \quad (1)$$

where $u \in \mathcal{U}$ describes the state of the system lying in a Hilbert space \mathcal{U} (for the sake of simplicity), A is a—possibly non-linear— operator modelling the physics of the system, and $f \in \mathcal{U}^*$ is some external influence (action / excitation / loading). Furthermore, we assume that the model depends on the parameter set $q \in \mathcal{Q}$ which is uncertain, and described in a tensor/matrix form. In other words, q is modelled as a $n \times n$ dimensional positive-definite matrix-valued random variable/field with finite second order moments

on a probability space $(\Omega, \mathfrak{F}, \mathbb{P})$ where Ω denotes the set of elementary events, \mathfrak{F} is a σ -algebra of events, and \mathbb{P} is a probability measure, i.e.

$$q(x, \omega) : \mathcal{G} \times \Omega \rightarrow \mathcal{S}^+(\mathbb{R}^{n \times n}). \quad (2)$$

Here

$$\mathcal{S}^+(\mathbb{R}^{n \times n}) := \{C \in \mathbb{R}^{n \times n} : C = C^T, \quad \mathbf{z}^T C \mathbf{z} > \mathbf{0}, \quad \forall \mathbf{z} \in \mathbb{R}^n \setminus \mathbf{0}\}. \quad (3)$$

Given uncertain q the system in Eq. (1) rewrites to the stochastic one:

$$A(q(x, \omega), u(x, \omega)) = f(x), \quad u(0) = u_0, \quad (4)$$

which further is to be solved for $u(x, \omega) \in \mathcal{U} \otimes L_2(\Omega, \mathfrak{F}, \mathbb{P})$. Note that in the previous equation the external influence f , as well as initial conditions u_0 can be also described as uncertain, and thus included in the parameter set. The theory presented further does not depend on this choice and is general enough to cover all of the mentioned cases.

Given that the response of the model is uncertain, all its relevant information may be obtained via corresponding stochastic description. Here we will focus on the r -th, $r \in \mathbb{N}$, central moment of $u \equiv u(x, \omega)$:

$$\mathbb{E}((u - \mathbb{E}(u))^r) = \int_{\Omega} (u - \mathbb{E}(u))^r \mathbb{P}(d\omega) \quad (5)$$

with $\mu(u) := \mathbb{E}(u)$ being the mean or the first raw moment and $\text{Var}(u) := \mathbb{E}((u - \mathbb{E}(u))^2)$ being the second central moment or the variance. The objective of this study is to determine these two moments after the appropriate discretization of the problem presented in Eq. (4).

Due to spatial and stochastic dependence, the solution u in Eq. (4) is first discretised in a spatial domain, i.e. we search for the solution in a finite subspace $\mathcal{U}_h \subset \mathcal{U}$. After rewriting the problem in Eq. (4) in a variational form, the spatial discretisation $u_h(\omega) \in \mathcal{U}_h$ — h being the discretization parameter—can take the finite element form on a sufficiently fine spatial grid \mathcal{T}_h ¹. The expectation functional in Eq. (5) then rewrites to:

$$\mathbb{E}((u_h - \mathbb{E}(u_h))^r) = \int_{\Omega} (u_h - \mathbb{E}(u_h))^r \mathbb{P}(d\omega), \quad (6)$$

in which the exact solution u is substituted by a semi-discretised solution $u_h \equiv u_h(\omega)$.

Due to the complexity in integrating the above equations analytically, in this paper, the focus is on the sampling-based Monte Carlo (MC) estimators [19, 9] that employ multi-level approximation of the finite element solution, also known as the multi-level Monte Carlo (MLMC) method [15, 11, 12]. However, the multi-level version of the MC algorithm as employed in the literature is based on the classical absolute error estimates, and therefore the convergence of the algorithm strongly depends on the solution magnitude. In this article, we propose a new version of the algorithm in which the statistical relative error is proposed. The new estimate is taken to be scale-invariant meaning that the solution magnitude does not affect the algorithm convergence.

¹Other types of discretization techniques can be considered as well

2.1. Monte Carlo estimation for the mean

Let $u_{h,N} := u_h(\omega_i), \{i = 1, \dots, N\}$, be the fully-discretized solution of Eq. (4), where N is the sample size. Further, let each sample $u_h(\omega_i)$ come from the identical distribution as $u_h(\omega)$. For the unbiased estimate of the statistic of $g(\omega)$, we take symmetric function

$$\mu^{\text{MC}}(g) = \frac{1}{N}(g(\omega_1) + g(\omega_2) + \dots + g(\omega_N)), \quad (7)$$

meaning that the estimate does not depend on the order in which observations were taken. The existence and uniqueness of such a choice are given in [14]. By use of Eq. (7) one may formulate the MC estimate of the mean $\mu(u_h)$ as

$$\mu^{\text{MC}}(u_{h,N}) := \frac{1}{N} \sum_{i=1}^N u_h(\omega_i). \quad (8)$$

Following this, the approximation error of the MC based mean estimate compared to the exact mean reads

$$\varepsilon = \mu^{\text{MC}}(u_{h,N}) - \mathbb{E}(u), \quad (9)$$

which further can be rewritten as

$$\varepsilon = \mu^{\text{MC}}(u_{h,N}) - \mathbb{E}(u_h) + \mathbb{E}(u_h) - \mathbb{E}(u). \quad (10)$$

The first term in the previous equation is the sampling error $\varepsilon_s := \mu^{\text{MC}}(u_{h,N}) - \mathbb{E}(u_h)$ defined by a central limit theorem

$$\varepsilon_s \sim \mathcal{N}\left(0, \frac{\text{Var}(u_h)}{N}\right), \quad (11)$$

whereas the second term describes the spatial discretization error

$$\varepsilon_d := \mathbb{E}(u_h) - \mathbb{E}(u).$$

Thus, the mean square error (MSE) reads

$$\varepsilon_{\text{MSE}}(\mu^{\text{MC}}(u_{h,N})) := \mathbb{E}((\varepsilon)^2) = \frac{\text{Var}(u_h)}{N} + (\mathbb{E}(u_h) - \mathbb{E}(u))^2. \quad (12)$$

Our particular interest lies in reducing the sampling part of the error ε_s that depends on the variance of the solution, and thus on its magnitude. Hence, if each observation $u_h(\omega_i)$ is scaled by a parameter c then the Monte Carlo error in Eq. (12) will be affected in a square proportional manner, which is not suitable in practical applications. To overcome this issue, we first assume that variance $\text{Var}(u_h)$ is known and define the new error estimate with the help of t-statistic [27, 8]:

$$e := \frac{\varepsilon}{\sqrt{\text{Var}(u_h)}} = \frac{\varepsilon}{\text{Std}(u_h)}, \quad (13)$$

where $\text{Std}(u_h)$ is the standard deviation of the solution. Hence, the substitute for the sampling error in Eq. (11) reads

$$e_s \sim \mathcal{N}\left(0, \frac{1}{N}\right), \quad (14)$$

and is dimensionless. In other words, the new type of error is scale-invariant under linear transformations of samples, which further makes e_s suitable candidate for the mean error estimator.

By normalizing Eq. (12) one obtains the squared error estimate

$$e_{\text{MSE}}(\mu^{\text{MC}}(u_{h,N})) := \mathbb{E}((e)^2) = \frac{1}{N} + \frac{(\mathbb{E}(u_h) - \mathbb{E}(u))^2}{\text{Var}(u_h)}, \quad (15)$$

in which the second term represents the square of the new normalized discretization error $e_d := \frac{\varepsilon_d}{\text{Std}(u_h)}$. As in general the variance $\text{Var}(u_h)$ and hence the standard deviation $\text{Std}(u_h)$ are not known but estimated, the error defined in Eq. (13) will take a slightly different form i.e.

$$e_B^{\text{MC}} = \frac{\varepsilon}{\sqrt{\text{Var}^{\text{MC}}(u_{h,N})}} = \frac{\varepsilon}{\text{Std}^{\text{MC}}(u_{h,N})}. \quad (16)$$

Here both variance $\text{Var}^{\text{MC}}(u_{h,N})$ and standard deviation $\text{Std}^{\text{MC}}(u_{h,N})$ estimators are determined by a MC procedure with N random draws. However, in such a case the use of symmetric function as in Eq. (7) does not lead to an unbiased estimator any more.

Following [14] from all unbiased estimators of variance, the only one that is symmetric and of minimum variance is given by

$$h_2^{\text{MC}}(u_{h,N}) := \frac{1}{N-1} \sum_{i=1}^N (u_h(\omega_i) - \mu^{\text{MC}}(u_h))^2. \quad (17)$$

This estimator is known as the second h-statistic and is further derived by [7] and implemented by [21]. Introducing the notion of power sum $S_r \equiv S_r(u_{h,N}) := \sum_{i=1}^N (u_h(\omega_i))^r$, the second h-statistic can be also written as

$$h_2^{\text{MC}}(u_{h,N}) = \frac{NS_2 - S_1^2}{N(N-1)}. \quad (18)$$

The substitution of Eq. (18) in Eq. (16) for $\text{Var}^{\text{MC}}(u_{h,N})$ results in obtaining the complete error estimate for the mean:

$$e^{\text{MC}} = \frac{\varepsilon}{\sqrt{h_2^{\text{MC}}(u_{h,N})}}. \quad (19)$$

2.2. Monte Carlo estimation for the variance

The previously derived estimate in Eq. (18) is characterized by an approximation error given as

$$\varepsilon_v = h_2^{\text{MC}}(u_{h,N}) - \text{Var}(u_h) + \text{Var}(u_h) - \text{Var}(u), \quad (20)$$

in which $\text{Var}(u)$ denotes the exact variance of the solution u . Here

$$\varepsilon_{vs} := h_2^{\text{MC}}(u_{h,N}) - \text{Var}(u_h) \quad (21)$$

and

$$\varepsilon_{vd} = \text{Var}(u_h) - \text{Var}(u) \quad (22)$$

are the sampling and discretization errors, respectively. Hence, the MSE of the variance estimator reads:

$$\varepsilon_{v\text{MSE}}(h_2^{\text{MC}}(u_{h,N})) := \mathbb{E}((\varepsilon_v)^2) = \text{Var}(h_2^{\text{MC}}(u_{h,N})) + (\text{Var}(u_h) - \text{Var}(u))^2. \quad (23)$$

Note that in contrast to the mean sampling error ε_s in Eq. (11), the variance sampling error ε_{vs} is not normally distributed anymore. The distribution type is application dependent and conditioned on the type of the distribution of u we sample from. Despite this, the mean and variance of the variance estimate are known in the general case, and our attention will be paid to these. The variance of the second order statistic is derived by [5] and reads

$$\mathbb{V}\text{ar}(\mathfrak{h}_2^{\text{MC}}(u_{h,N})) := \frac{1}{N} \left(\mu_4(u_h) - \frac{\mu_2(u_h)^2(N-3)}{(N-1)} \right), \quad (24)$$

where $\mu_2(u_h)$ and $\mu_4(u_h)$ represent the second and fourth central population moments. The unbiased approximation of fourth central moment $\mu_4(u_h)$ is computed by the fourth h-statistic [7]:

$$\begin{aligned} \mu_4(u_h) \approx \mathfrak{h}_4^{\text{MC}}(u_{h,N}) := & \frac{1}{N(N-1)(N-2)(N-3)} \left(-3S_1^4 + 6NS_1^2S_2 \right. \\ & \left. + (9-6N)S_2^2 + (-4N^2+8N-12)S_1S_3 + (N^3-2N^2+3N)S_4 \right), \end{aligned} \quad (25)$$

whereas the unbiased estimator of $\mu_2(u_h)^2$ is the polyache $\mathfrak{h}_{\{2,2\}}$ according to [29, 21], given as

$$\begin{aligned} \mu_2(u_h)^2 \approx \mathfrak{h}_{\{2,2\}}^{\text{MC}}(u_{h,N}) := & \frac{1}{N(N-1)(N-2)(N-3)} \left(S_1^4 - 2NS_1^2S_2 \right. \\ & \left. + (N^2-3N+3)S_2^2 + (4N-4)S_1S_3 + (-N^2+N)S_4 \right). \end{aligned} \quad (26)$$

Therefore, by substituting Eqs. (25) and (26) in Eq. (24), one obtains the unbiased estimate $\mathbb{V}\text{ar}^{\text{MC}}(\mathfrak{h}_2^{\text{MC}}(u_{h,N}))$ of $\mathbb{V}\text{ar}(\mathfrak{h}_2^{\text{MC}}(u_{h,N}))$. Another way of deriving is explained in [18], where an ansatz is initially considered, whose coefficients are determined by comparison between expectation of ansatz and Eq. (24).

For brevity, one may further rewrite Eq. (24) as

$$\mathbb{V}\text{ar}(\mathfrak{h}_2^{\text{MC}}(u_{h,N})) := \frac{\mathbb{V}_2(u_h)}{N}, \quad (27)$$

where

$$\mathbb{V}_2(u_h) := \mu_4(u_h) - \frac{\mu_2(u_h)^2(N-3)}{(N-1)}. \quad (28)$$

As in Eq. (23), only the term $\mathbb{V}\text{ar}(\mathfrak{h}_2^{\text{MC}}(u_{h,N}))$ is needed, the scale-invariant estimator will be defined only for this case. Hence, the new error estimate is given by normalizing Eq. (20) in the form:

$$e_v = \frac{\varepsilon_v}{\sqrt{\mathbb{V}_2(u_h)}}. \quad (29)$$

This further leads to

$$e_{v\text{MSE}}(\mathfrak{h}_2^{\text{MC}}(u_{h,N})) := \mathbb{E}((e_v)^2) = \frac{1}{N} + \frac{(\mathbb{V}\text{ar}(u_h) - \mathbb{V}\text{ar}(u))^2}{\mathbb{V}_2(u_h)}, \quad (30)$$

in which the first term is the scale-invariant sampling error e_{vs} , and the second term represents the dimensionless discretization error $e_{vd} := \frac{(\varepsilon_{vd})^2}{\mathbb{V}_2(u_h)}$. The sample based unbiased estimation of quantity $\mathbb{V}_2(u_h)$ is therefore determined by

$$\mathbb{V}_2^{\text{MC}}(u_{h,N}) := N \text{Var}^{\text{MC}}(h_2^{\text{MC}}(u_{h,N})). \quad (31)$$

Eqs. (12), (15), (23) and (30) signify that to attain an overall higher level of accuracy, one requires a very fine resolution of finite element mesh-grid, and a very large number of MC samples. This demands a tremendous amount of computational effort, making the algorithm practically unfeasible. Therefore, the desired moments are further estimated in a multi-level fashion following [15, 11, 12].

3. Multilevel Monte Carlo estimation for the mean

Let $\{l = 0, 1, 2, \dots, L\}$ be a generalised increasing sequence—in the context of decreasing the element size h —of nested mesh-grids \mathcal{T}_l , a regular (non-degenerate) partition of the computational domain \mathcal{G} of the problem described in Eq. (1). Here l denotes the mesh level, and L represents the finest mesh. Due to the linearity of the expectation operator, one may express the MLMC (also denoted by ML) mean estimate of the mean $\mu(u_{h_L})$ using a set of samples $\{N_l\} := \{N_0, N_1, \dots, N_L\}$ as [15]

$$\begin{aligned} \mu^{\text{ML}}(u_{h_L, \{N_l\}}) &:= \mu^{\text{MC}}(u_{h_0, N_0}) + \sum_{l=1}^L \mu^{\text{MC}}(u_{h_l, N_l} - u_{h_{l-1}, N_l}) \\ &= \sum_{l=0}^L \mu^{\text{MC}}(Y_{h_l, N_l}). \end{aligned} \quad (32)$$

Here $\mu^{\text{MC}}(u_{h_0, N_0})$ is the MC estimator of mean $\mu(u_{h_0})$ on level $l = 0$ using N_0 samples, and $\mu^{\text{MC}}(u_{h_l, N_l} - u_{h_{l-1}, N_l})$ represents the approximation of mean $\mu(u_{h_l, N_l} - u_{h_{l-1}, N_l})$ with $l > 0$ and N_l samples; $\mu^{\text{MC}}(Y_{h_l, N_l})$ is the MC estimator of $\mu(Y_{h_l})$ such that for $l = 0$, $Y_{h_0, N_0} = u_{h_0, N_0}$, otherwise $Y_{h_l, N_l} := u_{h_l, N_l} - u_{h_{l-1}, N_l}$. Note that each term Y_{h_l, N_l} , $l \geq 0$ is sampled independently, whereas for $l > 0$ the quantities u_{h_l, N_l} and u_{h_{l-1}, N_l} in Y_{h_l, N_l} are considered to be strongly correlated.

As the mean estimate on the finest grid $\mu^{\text{ML}}(u_{h_L, \{N_l\}})$ is obtained as the telescopic sum of the difference of MC mean estimates on the coarser grids, the MSE corresponding to Eq. (12) takes the form:

$$\varepsilon_{\text{MSE}}(\mu^{\text{ML}}(u_{h_L, \{N_l\}})) = \sum_{l=0}^L \frac{\text{Var}(Y_{h_l})}{N_l} + (\mathbb{E}(u_{h_L}) - \mathbb{E}(u))^2. \quad (33)$$

The above error consists of two terms, the variance of the estimator, given as ε_s and the square of spatial discretization error $\varepsilon_d := \mathbb{E}(u_{h_L}) - \mathbb{E}(u)$, similar to the MC error estimate. As the variance of the estimator is not scale-invariant, we suggest the new MSE estimate following Eq. (13):

$$e_{\text{MSE}}(\mu^{\text{ML}}(u_{h_L, \{N_l\}})) = \frac{1}{\text{Var}(u_{h_L})} \left(\sum_{l=0}^L \frac{\text{Var}(Y_{h_l})}{N_l} \right) + \frac{(\mathbb{E}(u_{h_L}) - \mathbb{E}(u))^2}{\text{Var}(u_{h_L})}. \quad (34)$$

However, the normalization term $\text{Var}(u_{h_L})$ in the previous equation is generally not known. Hence, under the assumption that for any value of l , $\text{Var}(u_{h_l})$ will be approximately constant [12, 6], one may substitute $\text{Var}(u_{h_L})$ with $\text{Var}(u_{h_0})$. Under the consideration that $h_2^{\text{MC}}(u_{h_0, N_0})$ is the MC estimator of $\text{Var}(u_{h_0})$, and by defining the MC variance estimate of $\text{Var}(Y_{h_l}) := \text{Var}(u_{h_l} - u_{h_{l-1}})$ via $h_2^{\text{MC}}(Y_{h_l, N_l})$, Eq. (34) therefore transforms to

$$e_{\text{MSE}}^{\text{MC}}(\mu^{\text{ML}}(u_{h_L, \{N_l\}})) = \frac{1}{h_2^{\text{MC}}(u_{h_0, N_0})} \left(\sum_{l=0}^L \frac{h_2^{\text{MC}}(Y_{h_l, N_l})}{N_l} \right) + \frac{(\mathbb{E}(u_{h_L}) - \mathbb{E}(u))^2}{h_2^{\text{MC}}(u_{h_0, N_0})}. \quad (35)$$

The first entity here stands for the scale-invariant multi-level sampling error e_s^{MC} , whereas the second term defines the dimensionless discretization error e_d^{MC} . Therefore, to attain an overall MSE of ϵ^2 , it is adequate to satisfy the conditions such as $e_s^{\text{MC}} < \epsilon^2/2$ and $e_d^{\text{MC}} < \epsilon^2/2$.

If $\mathcal{C}_l \equiv \mathcal{C}(Y_{h_l, N_l})$ is the computational cost of determining single MC sample of Y_{h_l, N_l} , then the overall cost of the estimator $\mu^{\text{ML}}(u_{h_L, \{N_l\}})$ is given as $\mathcal{C}(\mu^{\text{ML}}(u_{h_L, \{N_l\}})) := \sum_{l=0}^L N_l \mathcal{C}_l$. In this study, the focus is only on satisfying the condition of sampling error under the assumption that the optimal level L is known. The optimum number of samples N_l on each level l is evaluated by solving a constrained optimization problem. That is, for a given error $\epsilon^2/2$, the cost function

$$f(N_l) = \arg \min_{N_l} \sum_{l=0}^L \left(N_l \mathcal{C}_l + \tau \frac{h_2^{\text{MC}}(Y_{h_l, N_l})}{h_2^{\text{MC}}(u_{h_0, N_0}) N_l} \right) \quad (36)$$

is minimized. Thereby the optimal samples N_l are calculated as

$$N_l = \tau \left(\frac{h_2^{\text{MC}}(Y_{h_l, N_l})}{h_2^{\text{MC}}(u_{h_0, N_0}) \mathcal{C}_l} \right)^{\frac{1}{2}}, \quad (37)$$

where τ is the Lagrange multiplier, determined by

$$\tau \geq \frac{2}{\epsilon^2} \sum_{l=0}^L \left(\frac{h_2^{\text{MC}}(Y_{h_l, N_l}) \mathcal{C}_l}{h_2^{\text{MC}}(u_{h_0, N_0})} \right)^{\frac{1}{2}}. \quad (38)$$

Let us consider the positive constants $c_1, c_2, c_3, \alpha, \beta, \gamma$, given that $\alpha \geq \frac{1}{2} \min(\beta, \gamma)$ and assume that the following error bounds [11, 12]

$$\begin{aligned} |\mathbb{E}(u_{h_l}) - \mathbb{E}(u)| &\leq c_1 h_l^\alpha, \\ h_2^{\text{MC}}(Y_{h_l, N_l}) &\leq c_2 h_l^\beta, \\ \mathcal{C}_l &\leq c_3 h_l^{-\gamma}, \end{aligned} \quad (39)$$

hold. Then, there exists another positive constant c_4 , such that for any $0 < \epsilon < e^{-1}$, the MLMC error estimator satisfies $e_{\text{MSE}}^{\text{MC}}(\mu^{\text{ML}}(u_{h_L, \{N_l\}})) < \epsilon^2$, and the total computational cost is bound by

$$\mathcal{C}(\mu^{\text{ML}}(u_{h_L, \{N_l\}})) \leq \begin{cases} c_4 \epsilon^{-2}, & \beta > \gamma, \\ c_4 \epsilon^{-2(\log \epsilon)^2}, & \beta = \gamma, \\ c_4 \epsilon^{-2-(\gamma-\beta)/\alpha}, & \beta < \gamma. \end{cases} \quad (40)$$

3.1. Multilevel Monte Carlo estimation for the variance

To enhance the characterization of probabilistic system response, this paper also focuses on defining the MLMC estimator of $\mathbb{V}\text{ar}(u_{h_L})$ using h-statistics [18], expressed in the form:

$$h_2^{\text{ML}}(u_{h_L, \{N_l\}}) := h_2^{\text{MC}}(u_{h_0, N_0}) + \sum_{l=1}^L (h_2^{\text{MC}}(u_{h_l, N_l}) - h_2^{\text{MC}}(u_{h_{l-1}, N_l})). \quad (41)$$

Here $h_2^{\text{MC}}(u_{h_0, N_0})$ is the MC estimator of $\mathbb{V}\text{ar}(u_{h_0})$ with N_0 samples; $h_2^{\text{MC}}(u_{h_l, N_l})$ and $h_2^{\text{MC}}(u_{h_{l-1}, N_l})$ represent the MC estimation of $\mathbb{V}\text{ar}(u_{h_l})$ and $\mathbb{V}\text{ar}(u_{h_{l-1}})$ using N_l samples, respectively. For simplification, we introduce:

$$Z_{h_l, N_l} = \begin{cases} h_2^{\text{MC}}(u_{h_0, N_0}), & l = 0, \\ h_2^{\text{MC}}(u_{h_l, N_l}) - h_2^{\text{MC}}(u_{h_{l-1}, N_l}), & l > 0. \end{cases} \quad (42)$$

Note that, for $l > 0$, u_{h_l, N_l} and u_{h_{l-1}, N_l} in Z_{h_l, N_l} are determined using the same random seed. Thus, the expansion in Eq. (41) is rewritten as

$$h_2^{\text{ML}}(u_{h_L, \{N_l\}}) = \sum_{l=0}^L Z_{h_l, N_l}. \quad (43)$$

In correspondence to Eq. (23), the MSE of the estimator $h_2^{\text{ML}}(u_{h_L, \{N_l\}})$ takes the form:

$$\varepsilon_{v\text{MSE}}(h_2^{\text{ML}}(u_{h_L, \{N_l\}})) = \mathbb{V}\text{ar}(h_2^{\text{ML}}(u_{h_L, \{N_l\}})) + (\mathbb{V}\text{ar}(u_{h_L}) - \mathbb{V}\text{ar}(u))^2. \quad (44)$$

Under further consideration that the quantity Z_{h_l, N_l} , for $l \geq 0$, are sampled independently, one may express the first term in the above equation as

$$\mathbb{V}\text{ar}(h_2^{\text{ML}}(u_{h_L, \{N_l\}})) = \sum_{l=0}^L \mathbb{V}\text{ar}(Z_{h_l, N_l}), \quad (45)$$

in which the variance $\mathbb{V}\text{ar}(Z_{h_l, N_l})$ is further defined—similar to Eq. (27)—by $\mathbb{V}_{l,2}/N_l$. Therefore, Eq. (44) is reformulated to

$$\varepsilon_{v\text{MSE}}(h_2^{\text{ML}}(u_{h_L, \{N_l\}})) = \sum_{l=0}^L \frac{\mathbb{V}_{l,2}}{N_l} + (\mathbb{V}\text{ar}(u_{h_L}) - \mathbb{V}\text{ar}(u))^2. \quad (46)$$

Following the notion of power sum S_r defined in Section 2.1, here we introduce the bivariate power sum [21, 18]

$$S_l^{a,b} := \sum_{i=1}^N X_{h_l}^+(\omega_i)^a X_{h_l}^-(\omega_i)^b, \quad (47)$$

where $X_{h_l}^+(\omega_i)_{i=1, \dots, N_l} := X_{h_l, N_l}^+ = u_{h_l, N_l} + u_{h_{l-1}, N_l}$ and $X_{h_l}^-(\omega_i)_{i=1, \dots, N_l} := X_{h_l, N_l}^- = u_{h_l, N_l} - u_{h_{l-1}, N_l}$. Subsequently, the unbiased MC estimation of the quantity $\mathbb{V}_{l,2}$ in Eq. (45) reads:

$$\begin{aligned} \mathbb{V}_{l,2}^{\text{MC}} = & \frac{1}{(N_l - 3)(N_l - 2)(N_l - 1)^2 N_l} \left(N_l((-N_l^2 + N_l + 2)(S_l^{1,1})^2 \right. \\ & + (N_l - 1)^2(N_l S_l^{2,2} - 2S_l^{1,0} S_l^{1,2}) + (N_l - 1)S_l^{0,2}((S_l^{1,0})^2 - S_l^{2,0})) \\ & + (S_l^{0,1})^2((6 - 4N_l)(S_l^{1,0})^2 + (N_l - 1)N_l S_l^{2,0}) - \\ & \left. 2N_l S_l^{0,1}((N_l - 1)^2 S_l^{2,1} + (5 - 3N_l)S_l^{1,0} S_l^{1,1}) \right). \end{aligned} \quad (48)$$

Analogous to Eq. (12), the MSE in Eq. (46) is split into statistical error ε_{vs} —which is of the order $\mathcal{O}(N_l^{-1})$ —and square of deterministic bias $\varepsilon_{vd} := \text{Var}(u_{h_L}) - \text{Var}(u_h)$. As described in Eq. (31), the MSE $\varepsilon_{v\text{MSE}}$ is transformed to a scale-invariant version $e_{v\text{MSE}}$ by considering $\mathbb{V}_2(u_{h_L})$ as the normalization constant. However, we make an assumption that the value of $\mathbb{V}_2(u_{h_l})$ stays approximately close for all values of l , i.e., $\mathbb{V}_2(u_{h_L}) \approx \mathbb{V}_2(u_{h_0})$. If $\mathbb{V}_2^{\text{MC}}(u_{h_0, N_0})$ is the MC estimator of $\mathbb{V}_2(u_{h_0})$, then the new normalized MSE is given in the form:

$$e_{v\text{MSE}}^{\text{MC}}(h_2^{\text{ML}}(u_{h_L, \{N_l\}})) = \frac{1}{\mathbb{V}_2^{\text{MC}}(u_{h_0, N_0})} \left(\sum_{l=0}^L \frac{\mathbb{V}_{l,2}^{\text{MC}}}{N_l} \right) + \frac{(\text{Var}(u_{h_L}) - \text{Var}(u))^2}{\mathbb{V}_2^{\text{MC}}(u_{h_0, N_0})}. \quad (49)$$

Here the first term defines the scale-invariant sampling error e_{vs}^{MC} , and the second term is the normalized deterministic error e_{vd}^{MC} . Thus, the accomplishment of total MSE ϵ_v^2 is justified by ensuring that both errors e_{vs}^{MC} and e_{vd}^{MC} are lesser than $\epsilon_v^2/2$.

As the focus of this article is only on satisfying the constraint $e_{vs}^{\text{MC}} < \epsilon_v^2/2$, one may determine the samples N_l analogous to Eqs. (36)-(38) as

$$N_l = \frac{2}{\epsilon_v^2} \sum_{l=0}^L \left(\frac{\mathbb{V}_{l,2}^{\text{MC}} \mathcal{C}_l}{\mathbb{V}_2^{\text{MC}}(u_{h_0, N_0})} \right)^{\frac{1}{2}} \left(\frac{\mathbb{V}_{l,2}^{\text{MC}}}{\mathbb{V}_2^{\text{MC}}(u_{h_0, N_0}) \mathcal{C}_l} \right)^{\frac{1}{2}}. \quad (50)$$

Note that, here \mathcal{C}_l is the computational cost of evaluating one MC sample of u_{h_l, N_l} and u_{h_{l-1}, N_l} in the difference term Z_{h_l, N_l} , which is equivalent to determining the cost of Y_{h_l, N_l} in Eq. (36).

Let us introduce the positive constants $c_5, c_6, \alpha_v, \beta_v$, such that $\alpha_v \geq \frac{1}{2} \min(\beta_v, \gamma)$ and the error bounds [18]

$$\begin{aligned} |\text{Var}(u_{h_l}) - \text{Var}(u)| &\leq c_5 h_l^{\alpha_v}, \\ \mathbb{V}_{l,2}^{\text{MC}} &\leq c_6 h_l^{\beta_v}, \\ \mathcal{C}_l &\leq c_3 h_l^{-\gamma}, \end{aligned} \quad (51)$$

are satisfied. Thus, one may state that, for any $0 < \epsilon_v < e^{-1}$, the total MSE is bound by $e_{v\text{MSE}}^{\text{MC}}(h_2^{\text{ML}}(u_{h_L, \{N_l\}})) < \epsilon_v^2$ with a computational cost

$$\mathcal{C}(h_2^{\text{ML}}(u_{h_L, \{N_l\}})) \leq \begin{cases} c_7 \epsilon_v^{-2}, & \beta_v > \gamma, \\ c_7 \epsilon_v^{-2(\log \epsilon_v)^2}, & \beta_v = \gamma, \\ c_7 \epsilon_v^{-2-(\gamma-\beta_v)/\alpha_v}, & \beta_v < \gamma. \end{cases} \quad (52)$$

Here $c_7 > 0$ is a constant.

4. Application to linear elasticity

Let $\mathcal{G} \in \mathbb{R}^2$ be a two-dimensional bone geometry with smooth Lipschitz boundary Γ . The goal is to find the displacements $\mathbf{u} \in \mathbb{R}^2$ at a spatial point $x \in \mathcal{G}$, such that the equilibrium equations

$$\begin{aligned} -\text{div } \boldsymbol{\sigma}(x) &= \mathbf{f}(x), \quad \forall x \in \mathcal{G}, \\ \mathbf{u}(x) &= \mathbf{u}_0 = \mathbf{0}, \quad \forall x \in \Gamma_D, \\ \boldsymbol{\sigma}(x) \cdot \mathbf{n}(x) &= \mathbf{t}(x), \quad \forall x \in \Gamma_N, \end{aligned} \quad (53)$$

describing the linear-elastic behaviour, are fully satisfied. Here, $\boldsymbol{\sigma}(x)$ is the Cauchy stress tensor which belongs to the space of second order symmetric tensors $\mathcal{S}_2(\mathbb{R}^2) := \{\boldsymbol{\sigma} \in (\mathbb{R}^2)^{\otimes 2} : \boldsymbol{\sigma} = \boldsymbol{\sigma}^T\}$; $\mathbf{f}(x) \in \mathbb{R}^2$ is the body force; $\mathbf{t}(x) \in \mathbb{R}^2$ represents the surface tension on Neumann boundary $\Gamma_N \subset \Gamma$, and $\mathbf{n}(x) \in \mathbb{R}^2$ is the outward unit normal to Γ_N . For simplicity, an homogeneous boundary condition $\mathbf{u}_0 = \mathbf{0} \in \mathbb{R}^2$ is considered on the Dirichlet boundary $\Gamma_D \subset \Gamma$. We may also assume here $\Gamma_D \cap \Gamma_N = \emptyset$.

One may further describe the strain-displacement relation as

$$\boldsymbol{\varepsilon}(x) = \frac{1}{2} (\nabla \mathbf{u} + \nabla \mathbf{u}^T), \quad \forall x \in \mathcal{G}, \quad (54)$$

where $\boldsymbol{\varepsilon}(x) \in \mathcal{S}_2(\mathbb{R}^2)$ denotes infinitesimal second order symmetric strain tensor. Finally, the material constitutive equation is of the linear form:

$$\boldsymbol{\sigma}(x) = \mathbf{C} : \boldsymbol{\varepsilon}(x), \quad \forall x \in \mathcal{G}, \quad (55)$$

in which \mathbf{C} represents a fourth order positive-definite symmetric elasticity tensor. Here the notion of symmetry signifies the major ($C_{ijkl} = C_{klij}$) and minor symmetries ($C_{ijkl} = C_{jikl} = C_{ijlk}$). As a result, one can map a \mathbf{C} tensor to a second order tensor C , more generally known as the elasticity matrix. This reduced C matrix belongs to a family of ($n \times n$), here $n = 3$, real-valued positive-definite symmetric matrices:

$$\mathcal{S}^+(\mathbb{R}^{3 \times 3}) := \{C \in \mathbb{R}^{3 \times 3} : C = C^T, \mathbf{z}^T C \mathbf{z} > \mathbf{0}, \forall \mathbf{z} \in \mathbb{R}^3 \setminus \mathbf{0}\}. \quad (56)$$

Accordingly, conforming to Voigt notation, Eq. (55) transforms to $\boldsymbol{\sigma}(x) = C \cdot \boldsymbol{\varepsilon}(x)$, with $\boldsymbol{\sigma}(x) \in \mathbb{R}^3$ and $\boldsymbol{\varepsilon}(x) \in \mathbb{R}^3$ denoting the stress and strain vectors respectively.

Material law as described previously is complicated when highly heterogeneous and anisotropic material such as bone tissue is to be modelled. To include aleatoric uncertainty with heterogeneity in Eq. (55), the material properties have to be modelled as random and spatially dependent. In this paper, a probabilistic point of view is studied, by which the C matrix is modelled as a matrix-valued second-order random field $C(x, \omega)$ on a probability space $(\Omega, \mathcal{F}, \mathbb{P})$. In other words, the random elasticity matrix can be modelled as a mapping:

$$C(x, \omega) : \mathcal{G} \times \Omega \rightarrow \mathcal{S}^+(\mathbb{R}^{3 \times 3}). \quad (57)$$

Therefore, for a specific \hat{x} and $\hat{\omega}$, $C(\hat{x}, \hat{\omega})$ is a second-order symmetric tensor, the symmetry of which is not fully known. In practice, the usual assumption is that the elasticity matrix C globally follows a certain type of symmetry (e.g. isotropic, orthotropic, etc.), even though the experiments today cannot provide this information with full certainty. Thus, in this paper, we assume that the matrix C follows a specific type of symmetry only in the mean, whereas each of the realizations can be of arbitrary symmetry. The latter ones are not constrained in order to give our model a full degree of freedom. For instance, in a case when the predefined mean symmetry turned out to be incorrect, one would still be able to identify other types of symmetry given experimental data. This is, however, not the case if we would assume that each of the realizations is constrained. Mathematically, the previous idea is developed in [24, 25, 26].

Following this, we model the homogeneous mean matrix as $\mathbb{E}(C) = \overline{C} = Q^T Q$, in which the term $Q \in \mathbb{R}^{3 \times 3}$ represents an upper triangular matrix (Cholesky factor). To include the randomness in the model, one may extend the mean formulation to

$$C(x, \omega) = Q^T T(x, \omega) Q, \quad (58)$$

such that

$$\mathbb{E}(T(x, \omega)) = I \quad (59)$$

holds. Here $T(x, \omega)$ is a matrix-valued second-order random field residing in $\mathcal{S}^+(\mathbb{R}^{3 \times 3})$, the mean value of which is an identity matrix $I \in \mathbb{R}^{3 \times 3}$. In this manner, the mean behaviour is controlled by \bar{C} , whereas the uncertainty is governed by $T(x, \omega)$. To construct $T(x, \omega)$, one may use the maximum entropy optimization principle as described in [25]. The optimization is of constrained type as $T(x, \omega)$ is known to be positive definite random tensor specified by the mean in Eq. (59), and the finite second-order moment of its inverse [24]. To describe the random elasticity matrix given in Eq. (58), the parameters of $T(x, \omega)$ have to be chosen such that they fit the characteristics of $C(x, \omega)$. For example, the dispersion parameter of $T(x, \omega)$ i.e., $\delta_T := [0, 1]$ is chosen such that the following equation

$$\delta_C = \frac{\delta_T}{\sqrt{n+1}} \left[1 + \frac{(\text{tr}(\bar{C}))^2}{\text{tr}(\bar{C})^2} \right]^{1/2} \quad (60)$$

holds. Here $\delta_C := [0, 1]$ is the coefficient of dispersion of the elasticity matrix $C(x, \omega)$.

The description of material uncertainties via random elasticity matrix field $C(x, \omega)$ leads to the apparent transformation of a linear-elastic material model to a stochastic model. The aim is to determine the random displacement vector field $\mathbf{u}(x, \omega) : \mathcal{G} \times \Omega \rightarrow \mathbb{R}^2$. Therefore, the equilibrium equations are rewritten in the form:

$$\begin{aligned} -\text{div } \boldsymbol{\sigma}(x, \omega) &= \mathbf{f}(x), \quad \forall x \in \mathcal{G}, \omega \in \Omega, \\ \mathbf{u}(x, \omega) &= \mathbf{u}_0 = \mathbf{0}, \quad \forall x \in \Gamma_D, \omega \in \Omega, \\ \boldsymbol{\sigma}(x, \omega) \cdot \mathbf{n}(x) &= \mathbf{t}(x), \quad \forall x \in \Gamma_N, \omega \in \Omega, \end{aligned} \quad (61)$$

in which the boundary conditions and body forces $\mathbf{f}(x)$ remain deterministic. Further, the linearized kinematics relationship is transformed to

$$\boldsymbol{\varepsilon}(x, \omega) = \frac{1}{2} (\nabla \mathbf{u}(x, \omega) + \nabla \mathbf{u}(x, \omega)^T), \quad \forall x \in \mathcal{G}, \omega \in \Omega, \quad (62)$$

where $\nabla(\cdot)$ operator is taken in a weak sense. Finally, the constitutive law is represented by

$$\boldsymbol{\sigma}(x, \omega) = \mathbf{C}(x, \omega) : \boldsymbol{\varepsilon}(x, \omega), \quad \forall x \in \mathcal{G}, \omega \in \Omega. \quad (63)$$

By carrying out the variational formulation of the above stochastic partial differential equations on \mathcal{G} and further discretizing in a finite element setting, one searches for the solution $\mathbf{u}_h(\omega) : \mathcal{U}_h \times \Omega \rightarrow \mathbb{R}^2$ in a finite subspace \mathcal{U}_h as described in [22, 16]. More precisely, the goal of this study is to determine the total displacement scalar field in Euclidean norm i.e., $u_h^{(t)}(\omega) = \|\mathbf{u}_h(\omega)\|$. Henceforth, this article focuses on estimating the second order statistics such as the mean and variance of sampled response $u_{h,N}^{(t)} := [u_h^{(t)}(\omega_i)]_{i=1}^N$ using the scale-invariant MLMC.

5. Numerical results on 2D proximal femur

A two-dimensional proximal femur bone geometry with a body width of approximately 7cm and 21.7cm in total height is considered. Fig. 1 shows the boundary conditions where an in-plane uniform pressure load with a resultant load of 1500N is applied on top of the bone, and zero displacements are considered at the bottom [30]. The finite

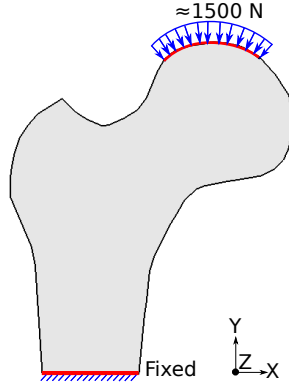


Figure 1: Boundary conditions

element method (FEM) based spatial discretization is undergone using four-noded plane stress elements. By sampling the probabilistic space, each deterministic simulation is thus executed by the finite element MATLAB based solver Plaston [22].

To implement the scale-invariant MLMC method, a sequence of four nested meshes with element size $h_{l-1} = 2h_l$ are considered (see Fig. 2). The corresponding mesh specifications are tabulated in Table 1. To this end, a matrix-valued random field $C(x, \omega)$, as described in Eq. (58), is modelled. A homogeneous mean matrix \bar{C} which belongs to the orthotropic material symmetry is taken into account as shown in Table 2 [1]. By setting the coefficient of dispersion of random elasticity matrix field to $\delta_C = 0.1$, the coefficient of dispersion of the matrix-valued random field $T(x, \omega)$ is determined using Eq. (60). Accordingly, the fluctuation matrix $T(x, \omega)$ is modelled as a non-linear transformation of 6 independent Gaussian random fields, each with zero mean and unit variance. Here, every standard Gaussian random field is discretized by the Karhunen-Loève expansion (KLE) which is truncated to a fixed 100 terms, and further defined by a Gaussian auto-correlation function with a correlation length of 3.5cm in the x and y-direction on all four levels of meshes [16, 22]. For more information on modelling the random field $T(x, \omega)$, see [22, 24, 25].

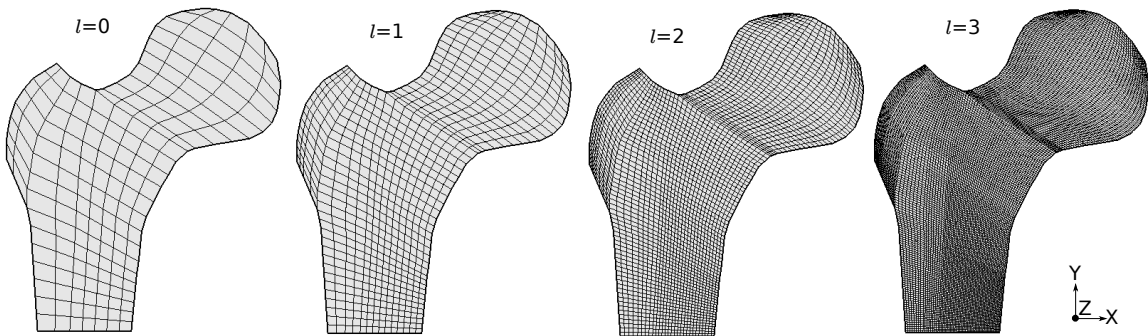


Figure 2: Nested mesh-grids of 2D femur bone

As mentioned in Section 4, the objective of the study is to compute the MLMC mean $\mu^{\text{ML}}(u_{h_L, \{N_l\}}^{(t)})$ and variance $h_2^{\text{ML}}(u_{h_L, \{N_l\}}^{(t)})$ estimates of the total displacement random field $u_{h_L}^{(t)}(\omega)$ on level $L = 3$. The corresponding mean and variance estimates are obtained for the sampling MSEs $\epsilon^2/2$ and $\epsilon_v^2/2$, respectively. To avoid the interpolation error, the terms $Y_{h_l, N_l}^{(t)}$ and $Z_{h_l, N_l}^{(t)}$ in Eqs. (32) and (42) are calculated only at finite element nodes

l	Elements	Nodes	DOF
0	171	206	396
1	684	753	1476
2	2736	2873	5688
3	10944	11217	22320

Table 1: Mesh specifications of 2D meshes

Young's modulus (N/cm ²)	Poisson's ratio	Shear modulus ((N/cm ²))
$E_1 = 12000 \times 10^2$	$\nu_{21} = 0.371$	$G_{12} = 5610 \times 10^2$
$E_2 = 20000 \times 10^2$		

Table 2: Orthotropic material parameters

which have the common spatial coordinates between all four levels of meshes. This further means that the MLMC mean and variance estimates of the system response on the finest level are evaluated only at these common nodes.

An apriori performance analysis of MLMC mean and variance estimators is done by the so-called screening test in which a fixed number of 50 samples is considered over four levels of meshes. Figs. 3 and 4 show the overview of corresponding results. Note that the results portrayed here are related only to a certain common node which corresponds to the maximum total displacement value at level $l = 0$. The top left and right plots in Fig. 3 show the behaviour of logarithmic MC mean and variance of quantities $u_{h_l,50}^{(t)}$ and $Y_{h_l,50}^{(t)}$ at each level l . The decay in $\mu^{\text{MC}}(Y_{h_l,50}^{(t)})$ describing the deterministic convergence and $h_2^{\text{MC}}(Y_{h_l,50}^{(t)})$ signifying stochastic convergence are certainly evident. On the other hand, the quantities $\mu^{\text{MC}}(u_{h_l,50}^{(t)})$ and $h_2^{\text{MC}}(u_{h_l,50}^{(t)})$ stay approximately constant at all values of l , as assumed in Section 3. The graph at the bottom displays the logarithmic computational time \mathcal{C}_l on each mesh level l . The corresponding values of \mathcal{C}_l are obtained by recording the timings for the considered 50 screening samples on a 2.3GHz Intel Core i5 processor with 8GB RAM by taking the average. As results show, computing becomes more expensive as the mesh refinement l increases.

Given Eq. (39) for the limit $l \rightarrow \infty$, $|\mathbb{E}(u_{h_l}) - \mathbb{E}(u)| \rightarrow 0$. This further implies via the triangle inequality that [6]

$$|\mathbb{E}(u_{h_l}) - \mathbb{E}(u_{h_{l-1}})| \leq c_8 h_l^\alpha, \quad (64)$$

in which $c_8 > 0$ is a constant. The constants in Eqs. (39) and (64) are evaluated by determining the slopes and y-intercepts of $\log|\mu^{\text{MC}}|$, $\log(h_2^{\text{MC}})$ and $\log(\mathcal{C}_l)$ in Fig. 3, and are further summarized in Table 3. Clearly the condition $\alpha \geq \frac{1}{2}\min(\beta, \gamma)$ is satisfied, and as $\beta < \gamma$, the computational complexity of MLMC mean estimate follows the third scenario in Eq. (40).

Fig. 4 depicts the deterministic convergence of logarithm of difference term $Z_{h_l,50}^{(t)}$ and the stochastic convergence of logarithmic $\mathbb{V}_{l,2}^{\text{MC}(t)}$ in the left and right plot, respectively. Also, the roughly constant behaviour of logarithmic variance estimate $h_2^{\text{MC}}(u_{h_l,50}^{(t)})$ and logarithm of $\mathbb{V}_2^{\text{MC}}(u_{h_l,50}^{(t)})$ can be seen in both the plots, reassuring the assumption made

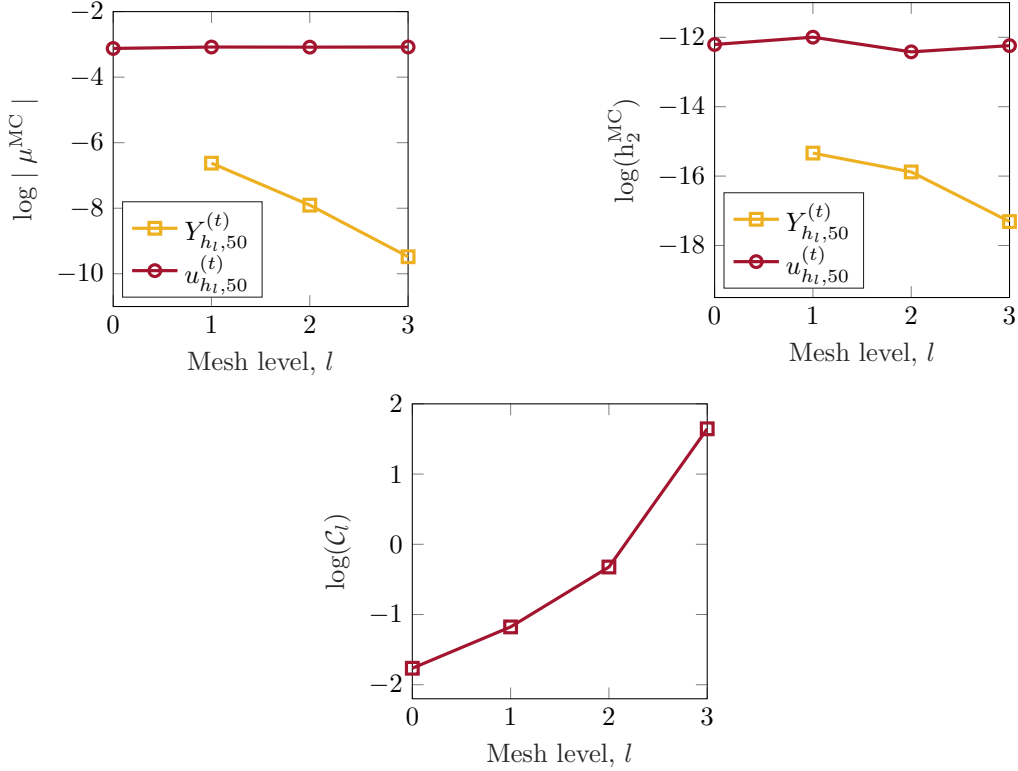


Figure 3: Screening results of MLMC mean estimator

α	β	γ	c_8	c_2	c_3
2.0594	1.4238	1.5989	0.0058	6.7907e-07	0.1265

Table 3: Convergence results of MLMC mean estimator

in Section 3.1. Corresponding to Eq. (51), let us suppose that when $l \rightarrow \infty$, there is a monotonic decay in $|\text{Var}(u_{h_l}) - \text{Var}(u)|$. Thereby, analogous to Eq. (64), the following condition

$$|\text{Var}(u_{h_l}) - \text{Var}(u_{h_{l-1}})| \leq c_9 h_l^{\alpha_v} \quad (65)$$

holds. The values of constants $c_9 > 0$ and α_v are tabulated in Table 4. In addition, the constants c_6 and β_v from Eq. (51) are also presented in the table. The constraint $\alpha_v \geq \frac{1}{2} \min(\beta_v, \gamma)$ and the case of $\beta_v < \gamma$ from Eq. (52) hold good.

α_v	β_v	c_9	c_6
1.6911	1.4741	1.1058e-06	1.1374e-11

Table 4: Convergence results of MLMC variance estimator

The performance results of scale-invariant MLMC are shown in Fig. 5. The left plot shows the propagation of a maximum number of samples $\max(N_l)$ on each level l for both MLMC mean and variance estimators, corresponding to errors $\epsilon^2/2$ and $\epsilon_v^2/2$, respectively. N_l decreases monotonically with increasing l for both the estimates. As the error estimates e_s^{MC} and e_{vs}^{MC} are fully normalized at the coarsest level $l = 0$, the values of N_0 for mean and variance estimates are much closer than the other levels. From this

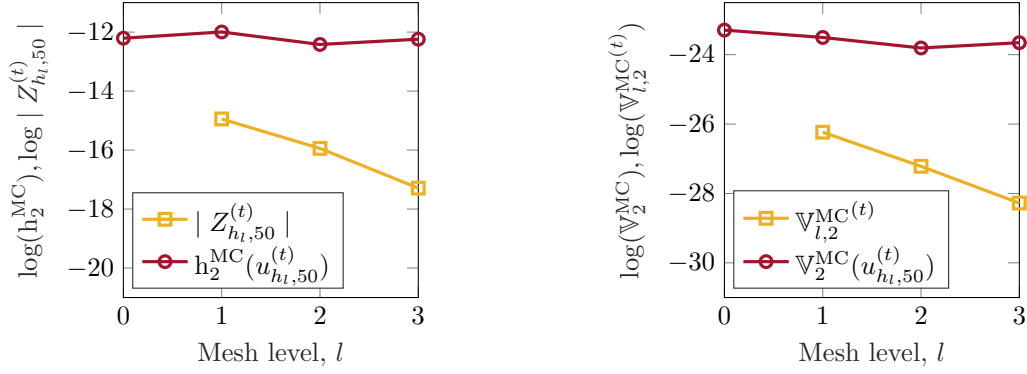


Figure 4: Screening results of MLMC variance estimator

figure, it is clear that the MLMC variance estimate requires more samples than the mean estimate for all the considered sampling MSEs. The right plot shows the overall cost of mean and variance estimation on level $L = 3$ by MLMC and MC against the user-specified normalized sampling MSEs. As the sampling part of MSE in Eqs. (15) and (30) are entirely scale-invariant, there is a non-asymptotic behaviour between the MC cost of mean and variance. However, the difference between the cost of MC and MLMC for both estimates is apparent, which is asymptotic. For all the considered MSEs, it is found that the MLMC mean and variance estimates are approximately 6 and 4 times faster than the classical MC mean and variance estimates, respectively. In other words, approximate cost savings of 83% and 75% are reported by the mean and variance MLMC estimates as compared to MC cost. Because of the use of scale-invariant error estimates in this study, we make a further observation that there is an asymptotic behaviour between the cost of MLMC mean and variance estimator, such that the mean converges faster than the variance against all the standardized errors.

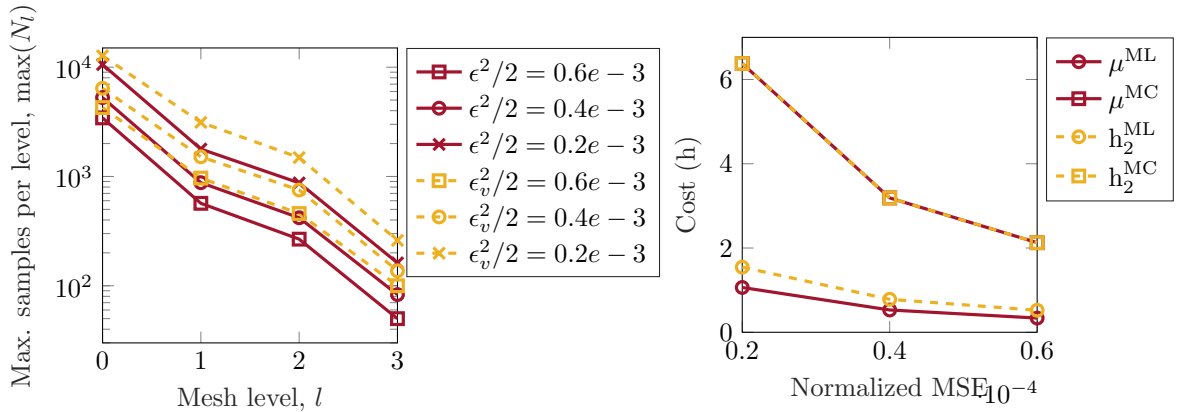


Figure 5: Performance of scale-invariant MLMC mean and variance estimators

Figs. 6 and 7 compare the mean and variance estimates of total displacement (TD) $u_{h_L, \{N_l\}}^{(t)}$ of human femur between MC and MLMC on mesh-grid $L = 3$. In general, the results are displayed for the normalized mean-squared accuracy of $0.2e-3$. Note that, as the displacement values are determined on the finest mesh $L = 3$ at the common nodes corresponding to the coarse mesh $l = 0$, the contour plots are mapped directly on this coarse mesh. In Fig. 6, a maximum mean value of approximately 0.046cm can be seen in the region of pressure load applied. Further, Fig. 7 shows the influence of material

uncertainty on the displacement $u_{h_L, \{N_l\}}^{(t)}$ due to the considered random material model $C(x, \omega)$. A maximum variance is witnessed at the top region of the bone. It is clear from both the figures that the difference in statistical results between both the methods is small.

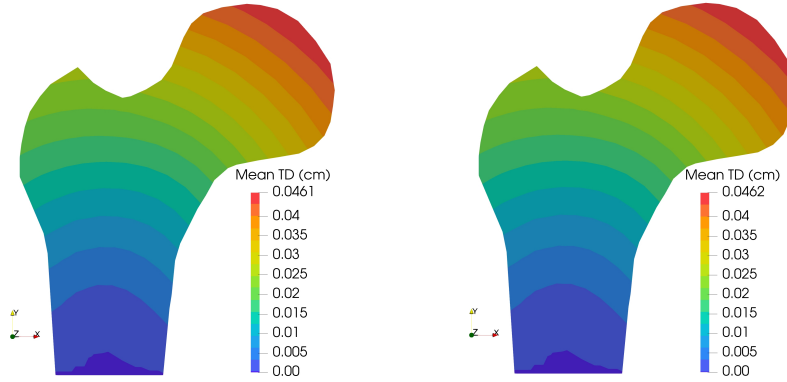


Figure 6: MLMC (on left) and MC (on right) mean estimate of total displacement

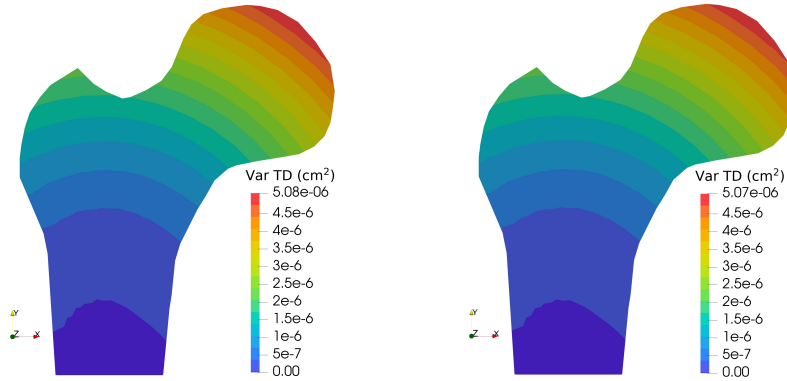


Figure 7: MLMC (on left) and MC (on right) variance estimate of total displacement

The summary of user-specified and accomplished normalized sampling errors of MLMC mean and variance estimators are tabulated in Table 5. In Eqs. (35) and (49), a fixed, maximum value of the normalization constant and number of samples N_l over the entire spatial domain are considered. As a result, the achieved sampling MSEs— e_s^{MC} and e_{vs}^{MC} —are the minimum at spatial points where the magnitude of total displacement is the lowest. Thus, the errors corresponding to the highest magnitude i.e., $\max(e_s^{\text{MC}})$ and $\max(e_{vs}^{\text{MC}})$, are presented in the table. It can be seen that the achieved maximum MSEs of mean and variance are within the user-specified limits of $\epsilon^2/2$ and $\epsilon_v^2/2$, respectively. Furthermore, the maximum absolute sampling MSEs corresponding to the obtained maximum scale-invariant errors are also presented in the table. The absolute MSEs of variance are much smaller as compared to the mean with no clear correlation between them. This emphasizes the need for normalized error estimates to ensure easier interpretation of the performance of MLMC estimators.

6. Conclusion

In this article, we propose a novel scale-invariant procedure for determining the MLMC mean and variance estimates. This is accomplished by normalizing the conventional absolute error estimates—used in the classical MLMC method—with the help of t-statistic.

User specified MSE, $\epsilon^2/2$	Achieved MSE, $\max(e_s^{\text{MC}})$	Achieved absolute MSE in cm^2
0.2e-3	0.197e-3	9.459e-10
0.4e-3	0.399e-3	1.889e-9
0.6e-3	0.598e-3	2.859e-9

(a) Mean

User specified MSE, $\epsilon_v^2/2$	Achieved MSE, $\max(e_{vs}^{\text{MC}})$	Achieved absolute MSE in cm^4
0.2e-3	0.198e-3	9.387e-15
0.4e-3	0.389e-3	1.856e-14
0.6e-3	0.583e-3	2.789e-14

(b) Variance

Table 5: User-specified and achieved sampling MSEs of MLMC estimates

When MLMC is implemented by minimizing the cost function, the scale-invariant approach helps in the easier specification of the input error. The algorithm reduces the ambiguity and makes the interpretation of performance analysis between the estimates easier. In addition, this procedure can also be utilized in making a cost comparison of individual estimates with different scales. This scale-invariant method is carried out on a linear-elastic material model of a two-dimensional proximal human femur by considering the uncertainties in the material description. Here the randomness in material characteristics is modelled—in a reduced parametric approach—by the random elasticity tensor/matrix-valued field. The input random model not only accommodates the heterogeneity of the material but also incorporates random anisotropy.

By propagating the material uncertainties to the output response (i.e., total displacement), the statistics like the mean and variance are estimated by the scale-invariant MC and MLMC algorithms. We observe that the MLMC variance estimate requires a higher number of samples than the mean estimate for all considered accuracies, thus, making the variance estimate more computationally expensive than the mean. On the other hand, in comparison to the MC cost of determining both estimates, the MLMC estimates outperform the MC. Due to the complete normalization, a non-asymptotic behaviour between the MC cost of mean and variance is witnessed for the considered standardized errors. On the contrary, the MLMC mean and variance costs follow an asymptotic path between them. Furthermore, the difference in the accuracy of mean and variance estimates between both the MLMC and MC methods is found to be small. The influence of the random material model on the total displacement is demonstrated via the estimated variance. The scale-invariant MLMC method can further be extended to other higher-order moments such as skewness and kurtosis.

References

- [1] R. Ashman, S. Cowin, W. Van Buskirk, and J. Rice. A continuous wave technique for the measurement of the elastic properties of cortical bone. *Journal of Biomechanics*, 17(5):349–361, Jan. 1984.
- [2] A. Barth, C. Schwab, and N. Zollinger. Multi-level Monte Carlo Finite Element method for elliptic PDEs with stochastic coefficients. *Numerische Mathematik*, 119(1):123–161, 2011.
- [3] C. Bierig and A. Chernov. Convergence analysis of multilevel Monte Carlo variance estimators and application for random obstacle problems. *Numerische Mathematik*, 130(4):579–613, Aug. 2015.
- [4] C. Bierig and A. Chernov. Estimation of arbitrary order central statistical moments by the multilevel Monte Carlo method. *Stochastics and Partial Differential Equations Analysis and Computations*, 4(1):3–40, Mar. 2016.
- [5] E. Cho and M. Cho. Variance of sample variance with replacement. *International Journal of Pure and Applied Mathematics*, 52:43–47, 01 2009.
- [6] K. A. Cliffe, M. B. Giles, R. Scheichl, and A. L. Teckentrup. Multilevel monte carlo methods and applications to elliptic pdes with random coefficients. *Computing and Visualization in Science*, 14(1):3–15, 2011.
- [7] P. S. Dwyer. Moments of Any Rational Integral Isobaric Sample Moment Function. *The Annals of Mathematical Statistics*, 8(1):21–65, 1937. Publisher: Institute of Mathematical Statistics.
- [8] R. A. Fisher. 043: Applications of "Student's" Distribution. *Metron*, 5:90–104, 1925.
- [9] G. Fishman. *Monte Carlo: Concepts, Algorithms, and Applications*. Springer Series in Operations Research and Financial Engineering. Springer-Verlag, New York, 1996.
- [10] D. Geraldès and A. Phillips. A comparative study of orthotropic and isotropic bone adaptation in the femur. *International Journal for Numerical Methods in Biomedical Engineering*, 30(9):873–889, 2014.
- [11] M. B. Giles. Multilevel monte carlo path simulation. *Operations Research*, 56(3):607–617, 2008.
- [12] M. B. Giles. Multilevel monte carlo methods. *Acta Numerica*, 24:259–328, 2015.
- [13] C. Graham and D. Talay. *Stochastic Simulation and Monte Carlo Methods: Mathematical Foundations of Stochastic Simulation*. Stochastic Modelling and Applied Probability. Springer-Verlag, Berlin Heidelberg, 2013.
- [14] P. R. Halmos. The Theory of Unbiased Estimation. *The Annals of Mathematical Statistics*, 17(1):34–43, 1946. Publisher: Institute of Mathematical Statistics.
- [15] S. Heinrich. Multilevel Monte Carlo Methods. In *Large-Scale Scientific Computing*, Lecture Notes in Computer Science, pages 58–67. Springer, 2001.

- [16] A. Keese. *Numerical Solution of Systems with Stochastic Uncertainties: A General Purpose Framework for Stochastic Finite Elements*. PhD thesis, Technische Universität Braunschweig, 2004.
- [17] T. S. Keller. Predicting the compressive mechanical behavior of bone. *Journal of Biomechanics*, 27(9):1159–1168, 1994.
- [18] S. Krumscheid, F. Nobile, and M. Pisaroni. Quantifying uncertain system outputs via the multilevel Monte Carlo method — Part I: Central moment estimation. *Journal of Computational Physics*, 414:109466, Aug. 2020.
- [19] N. Metropolis and S. Ulam. The Monte Carlo Method. *Journal of the American Statistical Association*, 44(247):335–341, 1949.
- [20] S. Mishra, C. Schwab, and J. Šukys. Multi-level Monte Carlo finite volume methods for nonlinear systems of conservation laws in multi-dimensions. *Journal of Computational Physics*, 231(8):3365–3388, Apr. 2012.
- [21] C. Rose and M. Smith. *Mathematical statistics with Mathematica.*, volume 481. New York, NY: Springer, 2002.
- [22] B. Rosić. *Variational formulations and functional approximation algorithms in stochastic plasticity of materials*. PhD thesis, Technische Universität Braunschweig, 2012.
- [23] V. Sansalone, D. Gagliardi, C. Desceliers, V. Bousson, J. Laredo, F. Peyrin, G. Haïat, and S. Naili. Stochastic multiscale modelling of cortical bone elasticity based on high-resolution imaging. *Biomechanics and Modeling in Mechanobiology*, 15(1):111–131, Feb 2016.
- [24] C. Soize. Maximum entropy approach for modeling random uncertainties in transient elastodynamics. *The Journal of the Acoustical Society of America*, 109(5):1979–1996, 2001.
- [25] C. Soize. Non-gaussian positive-definite matrix-valued random fields for elliptic stochastic partial differential operators. *Computer methods in applied mechanics and engineering*, 195(1):26–64, 2006.
- [26] C. Soize. Tensor-valued random fields for meso-scale stochastic model of anisotropic elastic microstructure and probabilistic analysis of representative volume element size. *Probabilistic Engineering Mechanics*, 23(2):307 – 323, 2008.
- [27] Student. The Probable Error of a Mean. *Biometrika*, 6(1):1–25, 1908. Publisher: [Oxford University Press, Biometrika Trust].
- [28] A. L. Teckentrup, R. Scheichl, M. B. Giles, and E. Ullmann. Further analysis of multilevel Monte Carlo methods for elliptic PDEs with random coefficients. *Numerische Mathematik*, 125(3):569–600, Nov. 2013.
- [29] D. S. Tracy and B. C. Gupta. Generalized h -Statistics and Other Symmetric Functions. *The Annals of Statistics*, 2(4):837–844, 1974. Publisher: Institute of Mathematical Statistics.

- [30] Z. Yosibash, R. Padan, L. Joskowicz, and C. Milgrom. A CT-Based High-Order Finite Element Analysis of the Human Proximal Femur Compared to In-vitro Experiments. *Journal of Biomechanical Engineering*, 129(3):297–309, June 2007.